

Mechanical Performance of Hybrid Graphene Nanoplates, Fly-Ash, Cement, Silica, and Sand Particles Filled Cross-Ply Carbon Fibre Woven Fabric Reinforced Epoxy Polymer Composites Beam and Column

Till Quadflieg¹, Vijay K. Srivastava², Thomas Gries¹ & Shantanu Bhatt¹

¹ Institut fuer Textiltechnik of RWTH Aachen University, Aachen, D-52074, Germany

² Department of Mechanical Engineering, Indian Institute of Technology (BHU), Varanasi-221005, India

Correspondence: Vijay K. Srivastava, Department of Mechanical Engineering, Indian Institute of Technology (BHU), Varanasi-221005, India. ORCID: <https://orcid.org/000001-6765-698500>. Tel: 91-542-236-9029. E-mail: vijayks210@gmail.com

Received: February 18, 2023

Accepted: April 6, 2023

Online Published: April 10, 2023

doi:10.5539/jmsr.v12n1p22

URL: <https://doi.org/10.5539/jmsr.v12n1p22>

Abstract

The main goal of this study is to reduce the brittleness of a fibre-reinforced cement base structure when exposed to the effects of graphene nanoplates, fly ash, silica, sand, and cement fillers to better understand the effect of hybrid nano/micro particle fillers on the mechanical performance of cross-ply carbon fibre reinforced epoxy resin composites. A three-point bending test through the width was used to measure flexural strength. The impact tests Izod at low impact velocity and Charpy through the thickness were used to determine the dynamic fracture strengths of pre-cracked and non-cracked composite samples. Also, the compressive test method was used to measure the compressive strength of hybrid particles and short glass fibre-reinforced epoxy resin composite square and circular columns. The results show compressive strength and flexural strength. Izod impact energy, Charpy impact energy, and dynamic fracture toughness of hybrid nano/microparticle-filled fibre composites have higher values than virgin fibre composites due to the influence of graphene nanoparticles and perfect interface bonding between two dissimilar molecules of nano and microparticles, which improve the fracture toughness and absorb impact energy. Overall, the results indicate that molecules of nano/microparticle-filled carbon fibre and glass fibre-reinforced epoxy resin composites can be used in aggressive environments because of the improved mechanical properties in comparison to the virgin fibre composites. In addition, SEM micrographs clearly indicate that nano- and microparticles are resistant crack propagation and deboned of matrix fibres.

Keywords: carbon fibre, graphene nanoplates, cement, sand, flyash, silica, mechanical properties, polymer composite

1. Introduction

Basically, cement-based structures have high compressive strength and low flexural strength compared to other materials. Moreover, cracks are one of the main problems due to their brittleness and lower durability. Generally, the damage and failure of concrete are caused by the nucleation of crack growth and debonding around the concrete and fibres. During the curing period of cement, a large quantity of calcium hydroxide (CH) crystals is developed due to the hydration process, which affects the bond between hydration products, increasing the deterioration of cement performance. The material containing SiO₂ reacts with CH to form C-S-H gel. The CH content in cement is reduced, the CH crystal size is refined, and the C-S-H content is increased, effectively improving the properties of cement-based composites (Li et al., 2021; Rico et al., 2017; Ahmad et al., 1995; Park et al., 2015; Nakaba et al., 2001). The main reason for crack formation is the random orientation of fibres and concrete in the cement matrix. The fibres and concrete cannot stop or prevent the initiation of microcracks in a cement matrix. Fibre-reinforced polymer is utilized to strengthen concrete structures because of its high strength-to-weight ratio and corrosion resistance (Papakonstantinofin et al., 2011; Wu et al., 2021). Interfacial fracture of fibre-reinforced polymer (FRP) concrete caused by flexural shear cracks determines the native materials, so it is necessary to know the FRP-concrete bond strength and failure load with the effect of concrete strength, FRP stiffness, effective bond length, and load displacement. Basically, the low toughness and tensile

strength of cement-based structures are the main causes of failures in infrastructure support. Recently, nanomaterials have provided effective approaches for improving the performance of concrete. Also, nanomaterials can modify the microstructure of the fibre-concrete interface, thereby improving the bond of the interface (Srivastava et al., 2017). The incorporation of microfibres into a cement matrix increases tensile strength, flexural strength and toughness. Carbon nanotubes (CNTs) and graphene nanosheets are widely used as reinforcements to improve the defects of cement-based materials at the nanoscopic level due to their large surface and ultra-high strength. Despite considerable progress in graphene-based cementitious composites, the biggest problem with graphene production is its low cost on an industrial scale (Li et al., 2017; Wang et al., 2022). The study shows that the addition of nanomaterials can improve cement-based compressive strength and enhance permeability. Graphene oxide (GO) is the oxidation reaction product of graphene, a mixture of functional groups with single sp² hybrid carbon, carboxyl, epoxy, and hydroxyl. It has a high specific surface area to show better performance in the hardened state of concrete. However, it is essential to find a more efficient and cost-effective way to apply graphene as a reinforcement in cement materials to increase the ductility, toughness, and strength of composite structures (Matsumaga et al., 2002). Also, fly ash particles are used as a fine mineral in concrete and can increase compactness due to fly ash and cement having the same organic compound of Al₂O₃, SiO₂, and Fe₂O₃. However, graphene oxide (GO) increased the activity of fly ash cement-based materials at a young age (Kayali et al., 1999; Zhau et al., 2022; Abdulla et al., 2016; Yuan et al., 2022; Arora et al., 2017; Wang et al., 1999). One of the latest methods of strengthening concrete is the use of glass fibres because of their high strength and resistance to weather and chemical attack (Jayannatha et al., 2015; Turla et al., 2014; Ling et al., 2020; Cao et al., 2014). The adhesive plays an important role in the perfect bonding of fibre and concrete (Golewski, 2018a; Golewski, 2018b). Therefore, epoxy resin is used to fill the open areas of fibres and concrete. The strengthening of concrete structures with epoxy resin-bonded fibre reinforcement provides good interface bonding between fibre and epoxy resin (Atmaca et al., 2017; Haruchansapong et al., 2014). The primary use of fibre-reinforced concrete polymer composites is to improve the tensile strength, crack resistance, fracture toughness, earthquake resistance, and ductility behaviour of structures under seismic load (Abbasi et al., 2016; Marques et al., 2010).

The above studies investigated the mechanical and physical properties of cement-based materials with nanomaterials and FRP (Guan et al., 2019; Shafiq et al., 2019; Assaedi et al., 2019). The primary goal of this research is to determine the effect of hybrid nano/microparticles (microparticle states; silica, fly ash, sand, and cement particles) on the compressive strength, flexural strength, Izod impact energy, Charpy impact inertia, and dynamic fracture toughness of cross-ply carbon fibre reinforced epoxy resin composites as measured by thickness, width, and pre-crack and un-crack specimens. The compressive strength of hybrid particles filled in short glass fibre-reinforced epoxy resin composites of short, long, square, and circular columns were measured, and their fractography was examined by SEM analysis.

2. Materials and Specimen Preparation

2.1 Materials and Preparation of GnPs Filled CFRP Composites

The matrix system used a two-part standard Epikote resin MGS RIMR-426 and hardener RIMH-433 thermosetting epoxies formulation. The ratio of resin to hardener was mixed at 100:26. The mixture is cured after 24 hours at a temperature of 20 degrees Celsius. First, 2 % graphene nanoplates were mixed with the resin and hardener before infiltration in the vacuum-created bag. Eight layers of cross-ply carbon fibre fabrics (300 x 300 mm) were laid down one by one on top of the glass sheet, with one layer of glass fibre fabric introduced in the middle of the eight layers of carbon fibre fabrics and fully covered with a plastic sheet to avoid the uniform flow of a mixture of graphene nanoplates (2 % GnPs) filled with resin and hardener in the ratio of 100:26 by the Vacuum Resin Transfer Molding (VRTM) process. The clamping force of the hot press is set to match exactly the post-injection pressure of 5 bars to ensure homogenous laminate thickness. Before injection, the two-part mixture of graphene nanoplates, resin, and hardener systems was stirred in a laboratory mixer and degassed after being homogeneously mixed. After injection, the mold was heated up by the press and kept at 90 °C for four hours to cure the laminates. The fabricated CFRP laminates with eight layers of carbon fibre fabrics were obtained, and it was cut into six pieces of the specimen as per the ASTM D-2344 standard size; length 210 mm and width 40 mm (Figure 1-a) from a circular diamond saw for the three-point bending test of pre-cracked length, 7mm and un-cracked through the width.

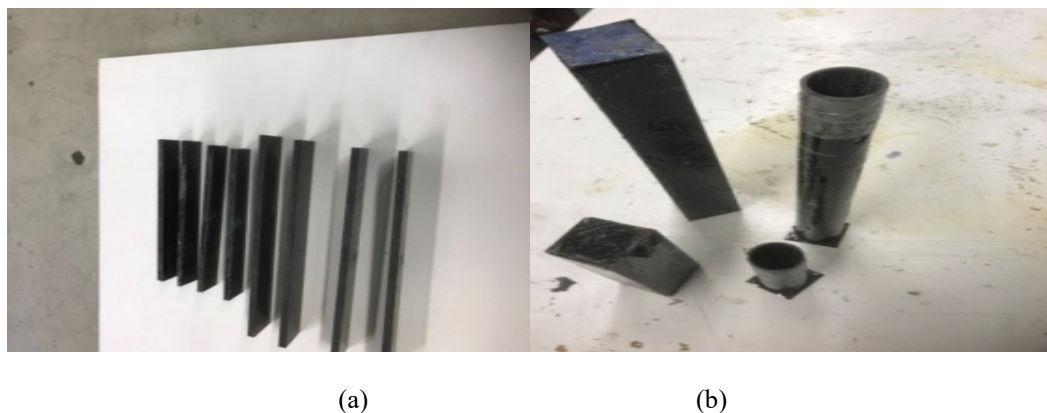


Figure 1. Fabricated composite specimens for (a) three point bending test specimens, and (b). fabricated short, long, Square and Circular Columns for compressive test

Table 1. Mechanical properties of materials (Li et al., 2021; Rico et al., 2017; Srivastava et al., 2017)

Materials	Grain size	Density	Elastic modulus GPa
Graphene Nanoplates (GnPs)	1.2 to 2.3 nm, 99% purity	2.3 g/cm ³	1000.0
Fly-ash (SiO ₂ , Al ₂ O ₃ , Fe ₂ O ₃ , CaO, MgO,	± 60 μm	540 g/m ³	98.0
Silica	5.5 nm	2.65 g/cm ³	73.0
Sand (SiO ₂)	0.06mm	1560 g/m ³	2.9
Cement (Al ₂ O ₃ , SiO ₂ , Fe ₂ O ₃ , Cao)	7-200 μm	1.44 g/cm ³	30.0
Cross-plyed Carbon Fibre	Diameter, 10μm	1.75 g/cm ³	228.0
Short Glass Fibre	Fibre dia., 10μm, fibre length ± 70 mm	2.53 g/cm ³	89.0
Epoxy Resin	Paste	1.7g/cm ³	2.0

2.2 Preparation of Hybrid Particles Filled CFRP Composites

The same epoxy resin (RIMR-426) and hardener (RIMH-433) were used. First, the ratio of each filler was fixed by the weight percentage of epoxy resin as per the reported work. To avoid the formation of voids, the graphene nanoplates (2 %), fly ash (2 %), silica (2 %), cement (2 %), and sand (4 %) particles were carefully mixed into the epoxy resin. The mechanical properties of materials are listed in Table 1. The thin layer of epoxy resin and filler mixture was spread on the top surface of the covered plastic sheet glass plate. Then, the first layer of cross-plyed carbon fibre fabric (350 x 350 mm) was put on top of the brick. The same method was repeated in each layer to build eight layers of carbon fibre fabrics. Also, one layer of epoxy resin-coated cross-ply carbon fibre strands and glass fibre was introduced after three layers of carbon fibre fabrics, and all areas of the glass plate sheet were covered with a plastic sheet on the top surface of eight layers. Finally, 10 kg of weight was put on top of the glass plate to remove the excess epoxy resin and filler mixture and allow it to cure for 24 hours. Cured composite laminates with a thickness of 8 mm were obtained and cut for the Charpy impact test from an ASTM D-7264 circular diamond saw with a length of 215.0 mm and a width of 18 mm. length: 90 mm, width: 18 mm, pre-crack length: 7 mm, and un-crack specimens were used for the Izod Impact test.

2.3 Preparation of Short, Long Square and Circular Columns

Cross-ply carbon fibre-reinforced epoxy resin composite mould was used to fabricate the square (40x40 mm) and circular (diameter 40 mm) shapes of mould columns as shown in Figure 1(b). First one layer of glass fibre fabric sheet was put inside the walls of the square and circular column moulds. Both square and circular moulds were filled with the homogenous mixture of graphene nanoplates (2 %), flash (2 %), silica (2 %), cement (2 %), and short glass fibre (30 %) reinforced epoxy resin sallows and left for 24 hours to cure the composite columns. The

weight percentage (%) of epoxy resin was used to determine the filler ratio. The dimensions of short (length = 150 mm), long (length = 310 mm), square, and circular columns were cut as per the ASTM C-39 M standard from a circular diamond saw for the compressive strength test. Length of circular and square columns: 305 mm; length of short square and circular columns: 150 mm, as shown in Figure 1(b).

3. Test procedures

3.1 Three Point Bending Test Through Width

Three-point bending test was performed on the Machine Z100 at the ITA. Testing Laboratory. The results are calculated according to DIN EN ISO 14125. A sharp notch length, 5 mm was cut into the centre top surface of the specimen, just below the loading point. The length of the support span was fixed at 160 mm, as shown in Figure 2(a). The pressure fin was mounted rigidly, and the test was carried out as per ASTM D-7264 and DIN EN ISO 14125 with a cross-head speed of 5 mm/min. All results of GnPs-filled CFRP thickness, 4.0 mm and hybrid particles-filled CFRP thickness, 8.0 mm composite specimens were recorded to show the variation in the applied centre force and mid-plane displacement of the composite specimens.

3.2 Compressive Test of Columns

The compressive test of the short, long square, and circular composite columns was carried out on the Machine Z100 as per ASTM 639M, as shown in Figure 2(b). The accuracy class according to DIN EN ISO 7500-1: see current calibration certificates the compressive load and displacement of all composite columns were measured using a force transducer: 100 kNXforce K (S/N: 152359/2001), a preload of 50 N, a force switch-off threshold of 10 % Fmax, an upper force limit of 90000 N, and a test speed of 5 mm/min.

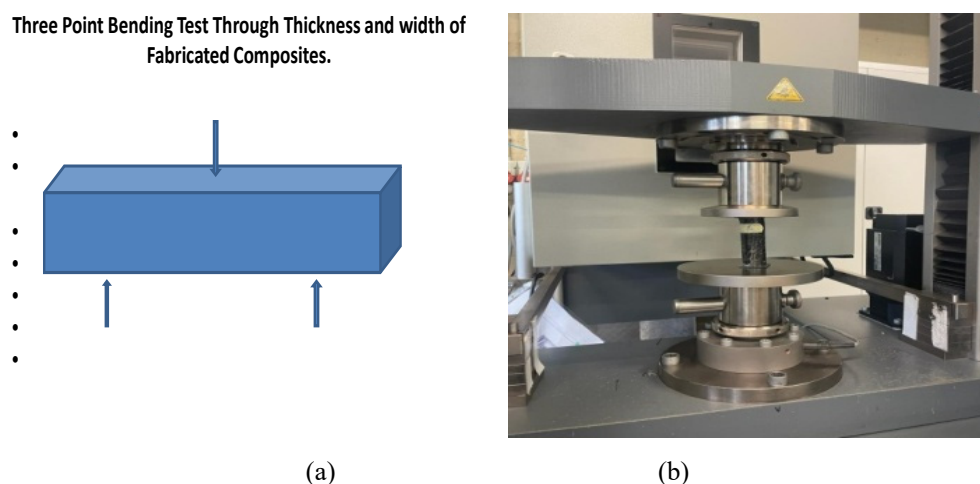


Figure 2. Arrangement of load under (a). Three point bending test, and (b). Experimental set-up of compressive test of Square and circular columns

3.3 Izod and Charpy Impact Tests of Composite Through Thickness

The Izod impact test specimen measures 90 mm in length, 18 mm in width, and 8 mm in thickness. The Izod impact test was performed through-thickness on un-cracked and pre-cracked (line crack length of 7 mm introduces through-thickness) composite specimens. The Charpy impact test specimen dimensions are length 215 mm, span length 160 mm, width 18 mm, and thickness 8.0 mm, respectively. Also, the Charpy impact test was performed on uncracked and pre-cracked (pre-crack length 4 mm through thickness) specimens through thickness under two-point support. The Izod and Charpy impact tests were performed with the equipment (Model; Resil Impactor-50, CEAST, S. p. A., Italy) as shown in Figure 3.



Figure 3. Resil Impactor-50 J, CEAST Instrument for Izod/Charpy Impact Tests

The impact hammer and vice lever with specimen adapter were used differently in the Izod and Charpy impact tests. The impact length and impact velocity were 0.327 m and 3.46 m/s. The Izod Impact and Charpy Impact energies were directly measured in terms of joules using the CEAT Instrument. Finally, the values of dynamic fracture toughness of cracked (K_{dtc}) and un-cracked (K_{dtu}) were calculated based on the experimentally obtained impact and Charpy impact energies of un-cracked and pre-cracked composite specimens using the following equations (1),

Dynamic fracture toughness of the cracked sample

$$K_{dtc} = \Delta E / (w-a) h \quad (1)$$

Dynamic fracture toughness of an uncracked sample

$$k_{dtu} = \Delta E / (w \times h) \quad (2)$$

where ΔE is the absorbing energy of materials measured during Izod and Charpy impact testing, and a , w , and h are the initial crack length, width, and thickness of the specimen, respectively.

3.4 Fractography Test

The scanning electron microscopy (SEM) test of fractured specimens was carried out at the central facility of the Scanning Electron Microscopy Laboratory, ITA, RWTH, Aachen University. SEM equipment was used for lateral resolution of up to circa 1 nm with a high depth of field. Integrated energy-dispersive. The x-ray microanalysis systems, or EDX, allow chemical analyses with a lateral sub-micrometer resolution for all elements with $Z > 4$ and detection limits > 0.1 weight percent. The electron probe microanalysis (EPMA) was used to focus high-energy electrons in the nm range onto the surface of the specimen to determine the thermal Schottky fields. The crystal structure and crystal orientation were examined to explain the phase contents, grain size, distributions, and deformation of materials.

4. Results and Discussion

4.1 Flexural Strength-Deflection Relationships

Based on the load-deflection responses for the GnP-filled CFRP composites and hybrid particle-filled CFRP composites of cracked and un-cracked specimens under the three-point bending test, the flexural strengths were recorded directly from the Universal testing machine as shown in Figures 4 and 5. The flexural strength under a three-point bending test can also be calculated from the given equation,

$$\text{Flexural Strength} = 1.5 \times F \times L / b d^2 \quad (3)$$

where F is the fracture load, L is the span length, and b and d are the specimen's width and depth. The measured deflections were located at the bottom of the middle span. These curves provided a valuable evaluation of the parameters reflecting the stiffness, strength, and flexure capacity of the specimen. All specimens show less deflection than the controls. It means that the uncracked specimens were stiffer than the pre-cracked specimens. Figure 4 depicts the trends of the flexural strength-displacement curve for the GnP carbon fibre reinforced epoxy resin. The flexural strength of uncracked GnP-filled CFRP and hybrid particle composites is linear until it reaches the maximum stress, at which point there is a sudden drop in stress, indicating brittle failure. The stress gradually decreases with increasing displacement in the pre-cracked GnP-filled CFRP composite and hybrid particle-filled CFRP composite up to the elastic limit and before half of the maximum flexural strength.

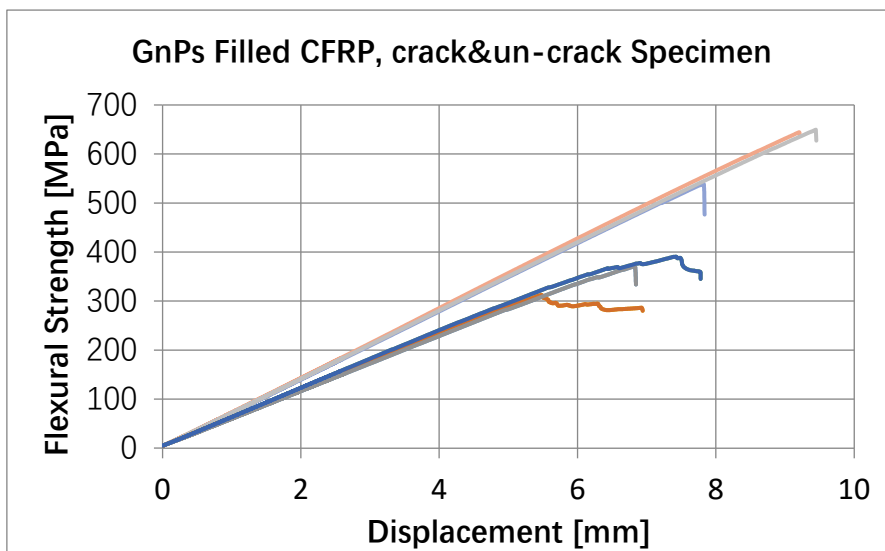


Figure 4. Variation of Strength with Displacement of graphene nanoplates filled CFRP composites (thickness=4.0 mm) cracked and un-cracked specimens

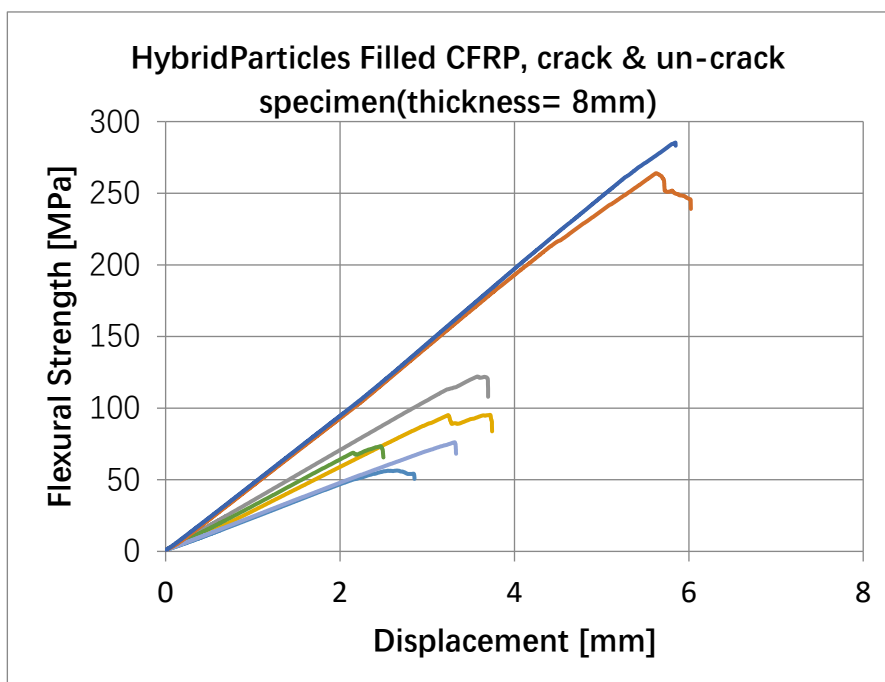


Figure 5. Variation of flexural strength with displacement of hybrid particles filled CFRP composites (thickness=8.0 mm) of pre-cracked and un-cracked specimens

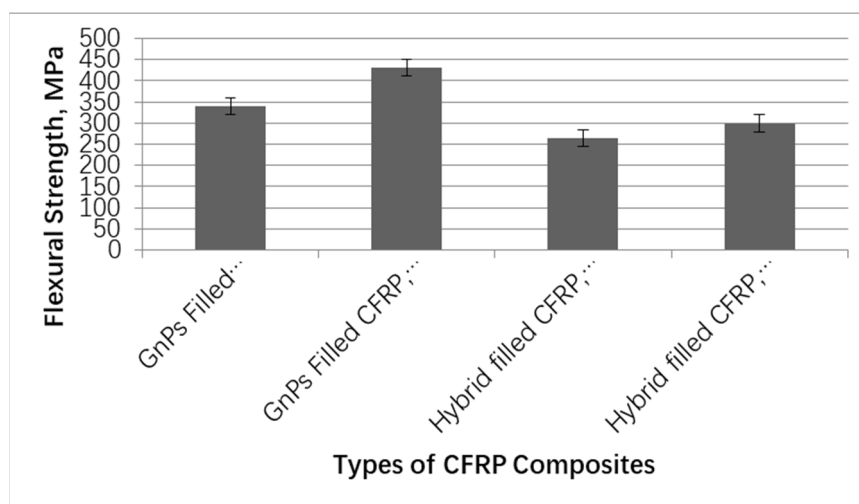


Figure 6. Variation of flexural strength of GnPs filled CFRP composites (thickness-4.5 mm) and hybrid parycles filled CFRP (thickness-8.0 mm) composite of pre-cracked and un-cracked specimens under three point bending test

The flexural strength of GnP-filled CFRP composites of pre-cracked and un-cracked specimens is 40 % higher than that of hybrid particles filled CFRP composites of un-cracked and pre-cracked specimens, as shown in Figure 6. This clearly indicates that the GnPs nanoparticle improved the toughness of CFRP composites due to the uniform dispersion of nanofillers, as shown in Figure 12(a). This improves the load-carrying capacity of the fibre-matrix interface and stops the crack propagation, crack bridging, or jumping of cracks to the next layer of fibre (Papakonstanfinon et al., 2011; Wu et al., 2021; Srivastava et al., 2017). The main reason is that the hybrid particles is not fully dispersed in the polymer matrix and agglurimated as can be identified from Figure 12(b) which decreases the flexural strength of polymer composites (Matsumaga et al., 2002; Kayali et al., 1999; Zhou et al., 2022). However, the composite material can still retain more load due to other layers that are yet to be debonded, delaminated, or failed. The influence of nano- and microparticles caused the composite to increase and decrease intermittently, as shown in Figure 12(c-d, e, f, g, and h). The distribution of fly ash and cement particles in the epoxy resin improves interface bonding along the carbon fibre direction (Kayali et al., 1999; Zhou et al., 2022). It was discovered that fly ash and cement particles essentially contain metal oxide and react with epoxy resin molecules, as shown in Figure 12(e-f) in their A, B, and C spherical forms. This significant improvement in flexural properties reflects the function of carbon fibre as the main load-carrying component of the composite material (Yuan et al., 2022; Arora et al., 2017). The graphene nanoplates and hybrid particle-filled epoxy resin hold the fibres together and also protect the fibres from delamination and debonding as shown in Figure 12 (d, g, and h).

4.2 Compressive Load-Displacement Relationship

The axial compression load-displacement curves of hybrid particles filled into short glass fibre-reinforced epoxy resin squares and circular short- and long-column composites are depicted in Figures 7 and 8. The peak load increases significantly as displacement increases. The compressive strengths of short (49.5 MPa), and long (70.0 MPa) circular composite columns are higher than those of short (28.5 MPa), and long (55.0 MPa) square composite columns and were directly obtained from the universal testing machine during tests, as shown in Figure 9.

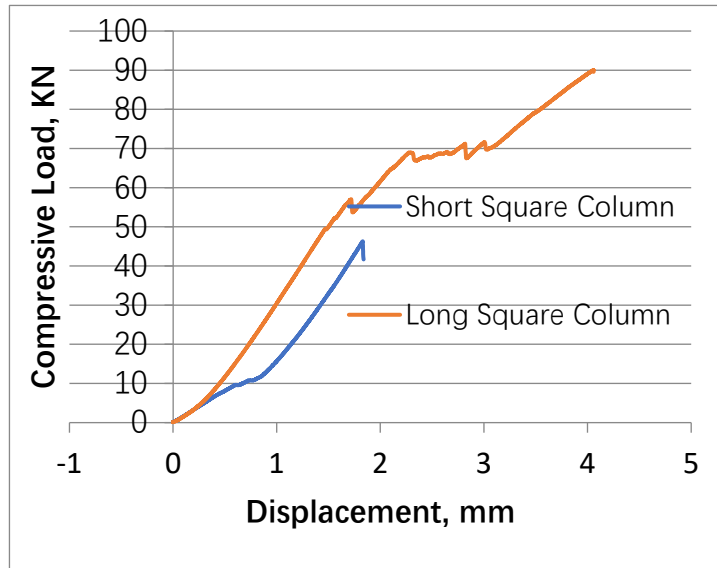


Figure 7. Variation of compressive load with displacement of square short and long square column

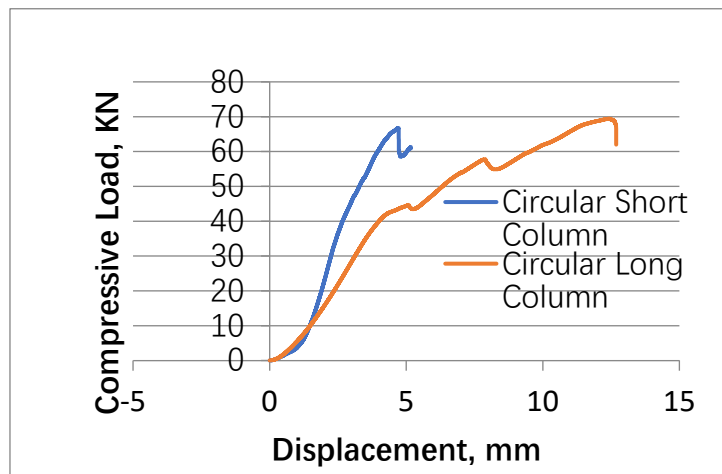


Figure 8. Variation of compressive load with displacement of circular short and long circular column

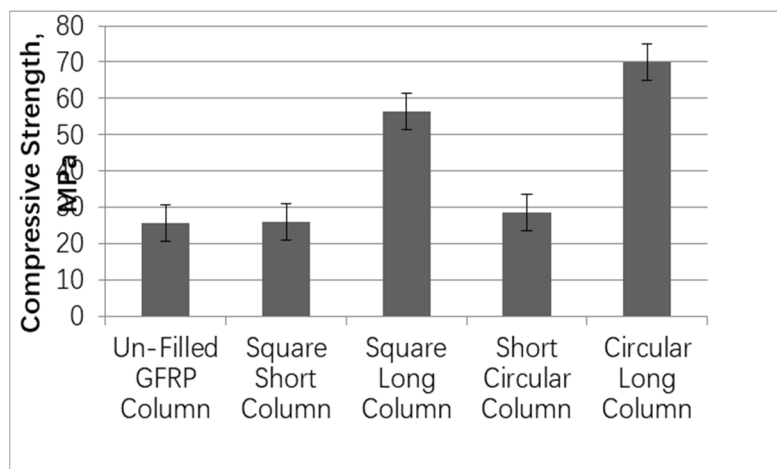


Figure 9. Variation of Compressive strength of square short. Long column and circular short, long columns of hybrid particles filled polymer composites

The compressive strength of the circular column is 20 % higher than the square column. The circular column has less buckling than the square column because it is centroidal and has symmetry about all axes, whereas the square column only has four axes of symmetry (Yuan et al., 2022; Wang et al., 1999). Also, the compressive strength calculated from equations 4 and 5 is given as a short circular column (50.95 MPa), a long circular column (55.73 MPa), a short square column (25.51 MPa), and a long square column (52.25 MPa). The difference between experimental and calculated values is approximately 12 %.

$$\text{Compressive Strength of circular column} = F/4 \times d^2 \quad (4)$$

$$\text{Compressive strength of square column} = F/a^2 \quad (5)$$

where F is the compressive force, d is the diameter of a circular column, and a is the length of all sides of the square.

It can be found that the compressive strength of short glass fibre reinforced epoxy resin composites (26.2 MPa) is increased by more than 30% by using hybrid particle fillers in the short glass fibre reinforced epoxy resin composites, mainly because short glass fibre is supported under the influence of hybrid particles, which improves the bearing capacity, as can be identified from Figure 12 (g and h). The slope of the load–displacement curve is the steepest, and the load-lifting rate is faster. This is because the axial compressive tests of hybrid columns are constrained by fibre composite materials, followed by the strength of the bending properties (Wang et al., 1999).

4.3 Izod Impact Energy and Charpy Impact Energy

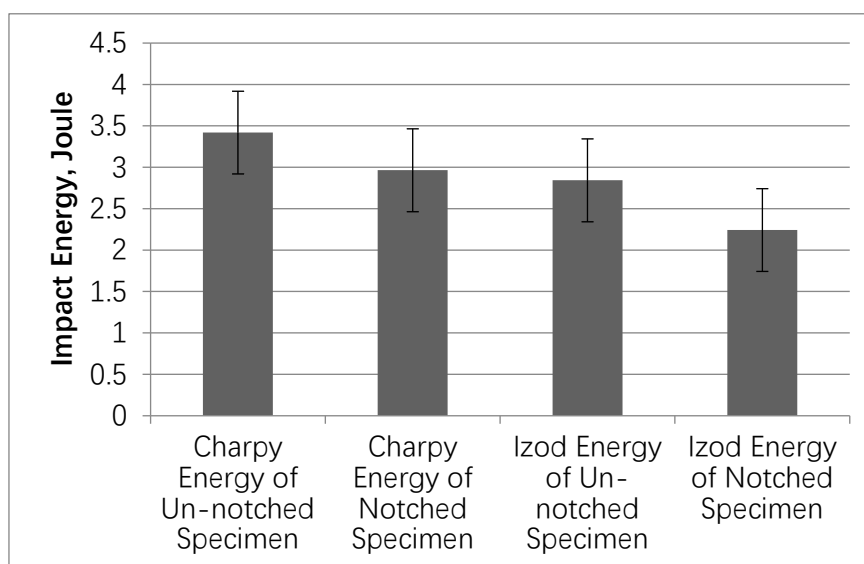


Figure 10. Variation of impact energy with pre-notch, un-notch hybrid particles filled CFRP composites under Izod and Charpy Impact tests

The essential function of an impact test is to get a "general" measure of the toughness or "fracture resistance" of a material by measuring the amount of energy required to break the specimen completely. Figure 10 depicts the variation of impact energy of hybrid particle-filled carbon fibre-reinforced epoxy resin composites through the thickness of pre-cracked and un-cracked specimens in Izod and Charpy impact tests. The Charpy impact energy of un-notch 3.46 joules and notch 3.0 joules hybrid particle-filled composites is greater than the Izod impact energy of un notch 2.5 joules and notch 2.25 joules hybrid particle-filled composites. The main reason for high Charpy impact energy values is that impact hammers strike at the specimen's midspan and gradually deform under a sudden load to delaminate fibre from the matrix and fracture, as shown in Figure 12 (c, d, e and f). Whereas, the Izod impact test involves striking a suitable test piece with a striker, mounted at the end of a pendulum. The test piece is clamped vertically with the notch facing the striker. The striker swings downward, impacting the ball at the bottom of its swing. Izod is a bending-type impact test that measures the total amount of energy required to fully break the fibre-matrix interface and the appearance of river-type brittle fractures in the resin reach area (see Figure

12 (e) and (f)). The Charpy and Izod impact methods allow for measuring the toughness and total energy dissipated in the material.

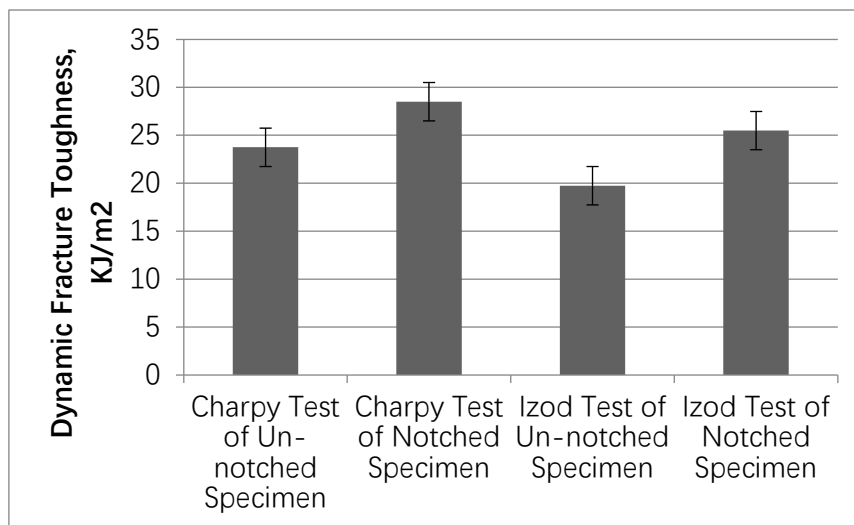


Figure 11. Variation of dynamic fracture toughness with pre-notch, un-notch hybrid particles filled CFRP composites under Izod and Charpy Impact tests

Figure 11 shows the variation of dynamic fracture toughness of un-notched and pre-notched hybrid particle-filled carbon fibre-reinforced epoxy resin composites. The results indicate that the dynamic fracture toughness of notch specimens under Charpy (28.5 KJ/m²) is lower than that under an Izod impact (25.0 KJ/m²). This does not allow us to know the plastic deformation around the crack tip. Generally, notched impact data reflect the energy required to propagate an existing crack through the specimen, whereas unnotched impact data will depend on both initiation and propagation energies (Abdulla et al., 2016; Yuan et al., 2022). The effect of fibres on the propagation of a crack through the hybrid-filled matrix is to increase the volume in which energy dissipation can take place. The presence of fibres also increases the absorbing capacity of potential energy (Turla et al., 2014).

5. Description

The experimental observations of GnPs-filled CFRP composite, hybrid particles-filled CFRP composite, and hybrid particles-filled short glass fibre composites under flexural, low-velocity impact, compressive, and micrographic loads clearly show that most of the curves dropped dramatically just after reaching the maximum strength under three-point bending and compressive loads, whereas fracture toughness and absorbed energy of CFRP composite are influenced by Izod/Charpy. This indicates that the hybrid particle-filled FRP composites behave as brittle materials due to the common organic compounds of sand, silica, fly ash, and cement. The hybrid constituent molecules strongly bond with the epoxy resin molecules, which can be attributed to the brittleness of the carbon fibres and glass fibres, whereas GnPs-filled CFRP composites increase the toughening and absorb more energy to propagate the cracks along the carbon fibre direction under bending stress and at low-velocity impact stress (Arora et al., 2017; Wang et al., 1999). The Charpy impact energy of hybrid particle-filled CFRP composites with an un-notch (3.49 joules) and pre-notch (2.58 joules) is higher than the Izod impact energy (2.54 joules un-notch and 2.26 joules pre-notch). This reflects the fact that the dynamic fracture toughness of pre-notch specimens under Charpy and Izod impact loads is higher than that of the un-notch specimens because stress wave energy is absorbed by the hybrid particles and is unable to propagate through the specimen (Jayannatha et al., 2015; Turla et al., 2014; Ling et al., 2020). The drop in flexural strength and dynamic fracture toughness in GnPs-filled CFRP and hybrid particles-filled CFRP and GFRP composites was attributed to their better mechanical properties (Cao et al., 2014; Golewski, 2018a). The fractography images depict the fracture behaviour of composites after bending, impact, and compressive tests; carbon fibre delaminated and debonded from the matrix, as shown in Figure 12(g) and (h). This demonstrates that crack propagation is angled with respect to the applied load in GnPs CFRP and hybrid particles CFRP and GFRP composites (Golewski, 2018b; Atmaca et al., 2017). Because circular columns have a high capacity to absorb compressive force due to the symmetry of centrifugal motion along all axes, the compressive strength of circular long (70 MPa) and short (49.5 MPa) composite columns is 20 % higher

than that of square long (55 MPa) and short (28.5 MPa) composite columns. Cracks typically begin in the resin reach area, propagate along the fibre direction, and debond the fibre from the matrix, as shown in Figure 12(g and h). This high improvement in the mechanical properties of GnP–cement composites can be attributed to the interaction between the GnPs and the epoxy resin paste. GnPs may have developed a good affinity or bond with the resin matrix, which can improve load-transfer capacity by absorbing energy more efficiently and offering better crack-spreading resistance (Srivastava et al., 2017; Li et al., 2017; Wang et al., 2020). GnP-filled CFRP composites have a bending strength of 430 MPa, while hybrid particle-filled CFRP composites have a bending strength of 300 MPa, which is less than that of GnP-filled CFRP composites. The GnPs nanoparticles enhanced the toughness of epoxy resin and increased the interface bonding with carbon fibre and epoxy resin (Golewski, 2018a; Golewski, 2018b; Atmaca et al., 2017). The incorporation of hybrid particles into the epoxy resin paste is more beneficial for its compressive than flexural strength (Haruchansapong et al., 2014; Abbasi et al., 2016). The compressive strength of the unfilled GFRP composite column was found to be 23.0 MPa and raised to a hybrid particle-filled GFRP 70 MPa for circular long column and 55 MPa for the square long column. Shear failure is always brittle in nature, which is not acceptable structural performance, especially in seismic conditions (Marques et al., 2010; Guan et al., 2019; Safiq et al., 2019; Assaedi et al., 2019).

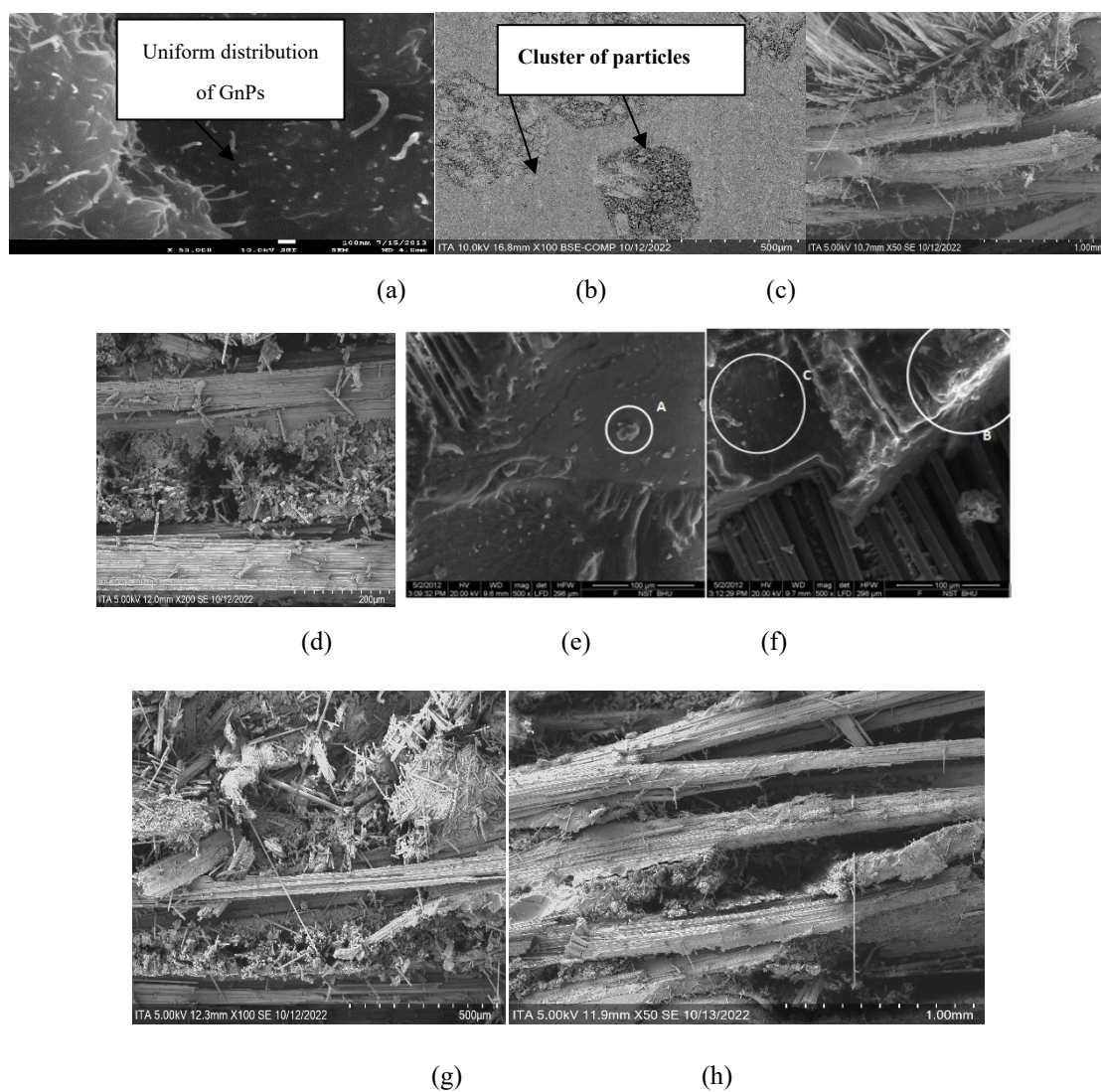


Figure 12. SEM micrographs of fractured samples showing the effects of hybrid particles in carbon fibre and short glass fibre reinforced polymer composites (a) cluster of particles, means agglomerated, (b) uniform dispersion of nanoparticles, (c) fibre broken, fibre deboned, (d) majority of fibre broken in between carbon fibre, (e) epoxy matrix fracture as indicated A, (f) crack propagated and debonded as indicated B and C, (g) short glass fibre surrounded by cluster of micro particles, and (h) carbon fiber broken and debonded

6. Concluding Remarks

Based on the aggressive experimental analysis of GnP-filled CFRP composites and hybrid particles-filled CFRP and GFRP composites under three-point bending, low-impact velocities, and compressive tests, the following conclusions can be drawn from this study.

- * The flexural strength of GnP-filled CFRP composites (un-cracked 430 kJ/m², pre-cracked 348 kJ/m²) is higher than that of hybrid particle-filled CFRP composites (un-cracked 300 kJ/m², pre-cracked 253 kJ/m²). Brittleness increased and bending strength decreased as a result of the agglomeration of hybrid particles.
- * The graphene nanoplate fillers in CFRP will also promote the interfacial interactions by establishing a chemical bonding network with epoxy resin as well as inducing the mechanical interlocking effect, which increases flexural strength.
- * Hybrid particle fillers reveal their considerable potential for improving the compressive strength, flexural strength, and energy-absorbing, durability of CFRP and GFRP polymer composites.
- * The compressive strength of a circular hybrid particle-filled short glass fibre composite column (70 MPa) has a higher value than that of a square hybrid particle-filled short glass fibre composite column (55 MPa) due to the less buckling of the circular column than the square column because the symmetry of the centroid is about all axes, whereas square columns have only 4 axes of symmetry.
- * The improved flexural strength, impact energy, dynamic fracture toughness, and compressive strength of FRP composites under the influence of nano- and microparticles motivate their application for seismic wave resistance.

Author Contributions

Based on the original experimental results manuscript is prepared and agreed to submit for the publication the original version of the manuscript.

Declaration of Conflicting Interests

The author(s) declared no potential conflicts of interest with respect to the research, authorship, and/or publication of this article.

Funding

The author(s) received no financial support for the research, authorship, and/or publication of this article.

References

- Ahmad, S. H., Xie, Y., & Yu, T. (1995). Shear ductility of reinforced lightweight concrete beams of normal strength and high strength concrete. *Cement and Concrete Composites*, 17(2), 147-159. [https://doi.org/10.1016/0958-9465\(94\)00029-X](https://doi.org/10.1016/0958-9465(94)00029-X)
- Abdulla, A. I., Razak, H. A., Salih, Y. A., & Ali, M. I. (2016). Mechanical properties of sand modified resins used for bonding CFRP to concrete substrates. *International Journal of Sustainable Built Environment*, 5(2), 517-525. <https://doi.org/10.1016/j.ijbsbe.2016.06.001>
- Atmaca, N., Abbas, M. L., & Atmaca, A. (2017). Effects of nano-silica on the gas permeability, durability and mechanical properties of high-strength lightweight concrete. *Construction and Building Materials*, 147, 17-26. <https://doi.org/10.1016/j.conbuildmat.2017.04.156>
- Sharma, S., & Arora, S. (2018). Economical graphene reinforced fly ash cement composite made with recycled aggregates for improved sulphate resistance and mechanical performance. *Construction and Building Materials*, 162, 608-612. <https://doi.org/10.1016/j.conbuildmat.2017.12.027>
- Abbasi, S. M., Ahmadi, H., Khalaj, G., & Ghasemi, B. (2016). Microstructure and mechanical properties of a metakaolinite-based geopolymer nanocomposite reinforced with carbon nanotubes. *Ceramics International*, 42(14), 15171-15176. <https://doi.org/10.1016/j.ceramint.2016.06.080>
- Assaedi, H., Alomayri, T., Shaikh, F., & Low, I. M. (2019). Influence of nano silica particles on durability of flax fabric reinforced geopolymer composites. *Materials*, 12(9), 1459. <https://doi.org/10.3390/ma12091459>
- Cao, P., Feng, D., Zhou, C., & Zuo, W. (2014). Study on fracture behavior of polypropylene fiber reinforced concrete with bending beam test and digital speckle method. *Computers and Concrete*, 14(5), 527-546. <https://doi.org/10.12989/cac.2014.14.5.527>

- Golewski, G. L. (2018a). Green concrete composite incorporating fly ash with high strength and fracture toughness. *Journal of cleaner production*, 172, 218-226. <https://doi.org/10.1016/j.jclepro.2017.10.065>
- Golewski, G. L. (2018b). Effect of curing time on the fracture toughness of fly ash concrete composites. *Composite Structures*, 185, 105-112. <https://doi.org/10.1016/j.compstruct.2017.10.090>
- Guan, J., Li, C., Wang, J., Qing, L., Song, Z., & Liu, Z. (2019). Determination of fracture parameter and prediction of structural fracture using various concrete specimen types. *Theoretical and Applied Fracture Mechanics*, 100, 114-127. <https://doi.org/10.1016/j.tafmec.2019.01.008>
- Haruehansapong, S., Pulngern, T., & Chucheepsakul, S. (2014). Effect of the particle size of nanosilica on the compressive strength and the optimum replacement content of cement mortar containing nano-SiO₂. *Construction and Building Materials*, 50, 471-477. <https://doi.org/10.1016/j.conbuildmat.2013.10.002>
- Jagannatha, T. D., & Harish, G. (2015). Influence of carbon & glass fiber reinforcements on flexural strength of epoxy matrix polymer hybrid composites. *International Journal of Engineering Research and Applications*, 5(4), 109-112.
- Kayali, O., Haque, M. N., & Zhu, B. (1999). Drying shrinkage of fibre-reinforced lightweight aggregate concrete containing fly ash. *Cement and concrete research*, 29(11), 1835-1840. [https://doi.org/10.1016/S0008-8846\(99\)00179-9](https://doi.org/10.1016/S0008-8846(99)00179-9)
- Li, Y., Liu, Y., & Wang, R. (2021). Evaluation of the elastic modulus of concrete based on indentation test and multi-scale homogenization method. *Journal of Building Engineering*, 43, 102758. <https://doi.org/10.1016/j.jobe.2021.102758>
- Li, X., Liu, Y. M., Li, W. G., Li, C. Y., Sanjayan, J. G., Duan, W. H., & Li, Z. (2017). Effects of graphene oxide agglomerates on workability, hydration, microstructure and compressive strength of cement paste. *Construction and Building Materials*, 145, 402-410. <https://doi.org/10.1016/j.conbuildmat.2017.04.058>
- Ling, Y. F., Zhang, P., Wang, J., & Shi, Y. (2020). Effect of sand size on mechanical performance of cement-based composite containing PVA fibers and nano-SiO₂. *Materials*, 13(2), 325. <https://doi.org/10.3390/ma13020325>
- Matsunaga, T., Kim, J. K., Hardcastle, S., & Rohatgi, P. K. (2002). Crystallinity and selected properties of fly ash particles. *Materials Science and Engineering: A*, 325(1-2), 333-343. [https://doi.org/10.1016/S0921-5093\(01\)01466-6](https://doi.org/10.1016/S0921-5093(01)01466-6)
- Marques, A. S., Amaral, P. M., Rosa, L. G., & Fernandes, J. C. (2010). Study of aggregate size effect on fracture toughness of petreousmacrocomposites (concrete). In *Materials Science Forum* (Vol. 636, pp. 1342-1348). Trans Tech Publications Ltd. <https://doi.org/10.4028/www.scientific.net/MSF.636-637.1342>
- Nakaba, K., Kanakubo, T., Furuta, T., & Yoshizawa, H. (2001). Bond behavior between fiber-reinforced polymer laminates and concrete. *Structural Journal*, 98(3), 359-367. <https://doi.org/10.14359/10224>
- Park, K., Ha, K., Choi, H., & Lee, C. (2015). Prediction of interfacial fracture between concrete and fiber reinforced polymer (FRP) by using cohesive zone modeling. *Cement and Concrete Composites*, 63, 122-131. <https://doi.org/10.1016/j.cemconcomp.2015.07.008>
- Papakonstantinou, C. G., Balaguru, P. N., & Auyeung, Y. (2011). Influence of FRP confinement on bond behavior of corroded steel reinforcement. *Cement and Concrete Composites*, 33(5), 611-621. <https://doi.org/10.1016/j.cemconcomp.2011.02.006>
- Rico, S., Farshidpour, R., & Tehrani, F. M. (2017). State-of-the-art report on fiber-reinforced lightweight aggregate concrete masonry. *Advances in Civil Engineering*, 2017. <https://doi.org/10.1155/2017/8078346>
- Srivastava, V. K., Gries, T., Veit, D., Quadflieg, T., Mohr, B., & Kolloch, M. (2017). Effect of nanomaterial on mode I and mode II interlaminar fracture toughness of woven carbon fabric reinforced polymer composites. *Engineering Fracture Mechanics*, 180, 73-86. <https://doi.org/10.1016/j.engframech.2017.05.030>
- Shafiq, N., Kumar, R., Zahid, M., & Tufail, R. F. (2019). Effects of modified metakaolin using nano-silica on the mechanical properties and durability of concrete. *Materials*, 12(14), 2291. <https://doi.org/10.3390/ma12142291>
- Turla, P., Kumar, S. S., Reddy, P. H., & Shekar, K. C. (2014). Processing and flexural strength of carbon fiber and glass fiber reinforced epoxy-matrix hybrid composite. *International Journal of Engineering Research and Technology (IRJET) Volume*, 3.

- Wu, S., Qureshi, T., & Wang, G. (2021). Application of graphene in fiber-reinforced cementitious composites: A review. *Energies*, *14*(15), 4614. <https://doi.org/10.3390/en14154614>
- Wang, X., Ding, S., Qiu, L., Ashour, A., Wang, Y., Han, B., & Ou, J. (2022). Improving bond of fiber-reinforced polymer bars with concrete through incorporating nanomaterials. *Composites Part B: Engineering*, *239*, 109960. <https://doi.org/10.1016/j.compositesb.2022.109960>
- Wang, T. W. H., Blum, F. D., & Dharani, L. R. (1999). Effect of interfacial mobility on flexural strength and fracture toughness of glass/epoxy laminates. *Journal of materials science*, *34*, 4873-4882.
- Yuan, X., Dai, M., Li, M., Zhang, S., & Zhang, M. (2022). Effect of Graphene Oxide and Fly Ash on Frost Resistance of the Steel Fiber Reinforced Concrete. *Sustainability*, *14*(10), 6236. <https://doi.org/10.3390/su14106236>
- Zhou, S., Zhang, X., Zhou, H., & Li, D. (2022). Effects of Graphene Oxide Encapsulated Silica Fume and Its Mixing with Nano-Silica Sol on Properties of Fly Ash-Mixed Cement Composites. *Crystals*, *12*(2), 144. <https://doi.org/10.3390/cryst12020144>

Copyrights

Copyright for this article is retained by the author(s), with first publication rights granted to the journal.

This is an open-access article distributed under the terms and conditions of the Creative Commons Attribution license (<http://creativecommons.org/licenses/by/4.0/>).